

## **Ka-BAND KLOPFENSTEIN TAPERED IMPEDANCE TRANSFORMER FOR RADAR APPLICATIONS**

**L. Resley and H. Song\***

Department of Electrical and Computer Engineering, University of Colorado, 1420 Austin Bluffs Parkway, Colorado Springs, CO 80918, United States

**Abstract**—The design, fabrication, and characterization of an amulti-section impedance transformer using Klopfenstein tapering method is presented. The transformer is employed in a Ka-band traveling-wave tube (TWT) for radar applications. The Klopfenstein tapering provides the shortest length between the two different impedance levels with continuous tapering sections.

### **1. INTRODUCTION**

In helix-TWT amplifiers, a highly-efficient matching output section is required in order to extract maximum power generated in the helix-TWT circuit. To realize this, a transformer is required between the helix circuit and the pillbox window for impedance matching. For compact helix-TWTs, the transformer should yield the shortest length with superior impedance matching characteristics.

The Klopfenstein taper is an impedance matching Dolph-Tchebycheff transmission line taper designed to minimize the reflections over a particular passband. The benefit of this design versus other transformers is that there is no wavelength dependent length requirement, which enables the taper design to be tailored to physical constraints of a transmission line structure. The Klopfenstein taper is an optimum transformer that provides lowest reflection coefficient over the passband and yields the shortest matching section, thereby allowing the device to be as compact as possible. The investigated Klopfenstein-tapered transformer waveguide includes a segmented transmission line of several sections to create a piecewise taper and then smoothed out to create the continuous taper.

---

*Received 23 November 2011, Accepted 2 March 2012, Scheduled 9 March 2012*

\* Corresponding author: Hoyoung Song (hsong@eas.uccs.edu).

In this paper, the Klopfenstein transformer was employed in the helix-TWT for radar applications. The Klopfenstein transformer is located between the pillbox window and the helix-TWT circuit. The pillbox window includes a cylindrical waveguide between two symmetrically shaped WR-28 waveguides. At the center of the cylindrical waveguide is a ceramic disk, which serves as an RF dielectric window. The Klopfenstein transformer is optimized to match the impedances of the pillbox window and the helix-TWT structure. The helix-TWT includes three dielectric support rods, a fifteen-turn helix coil, and a cylindrical vacuum cavity. The design, fabrication, and characterization of the transformer are described in the following sections.

## 2. THEORY AND DESIGN OF A KLOPFENSTEIN TRANSFORMER

Different types of tapers have different passband characteristics. A taper transition, which has characteristic impedance that varies continuously and smoothly from one impedance section to another, is an alternative to a multi-section quarter-wave transformer. In this study, we examined the Klopfenstein tapered transformer and implement this between the pillbox window and helix-TWT circuit to achieve impedance matching in the shortest possible length. The

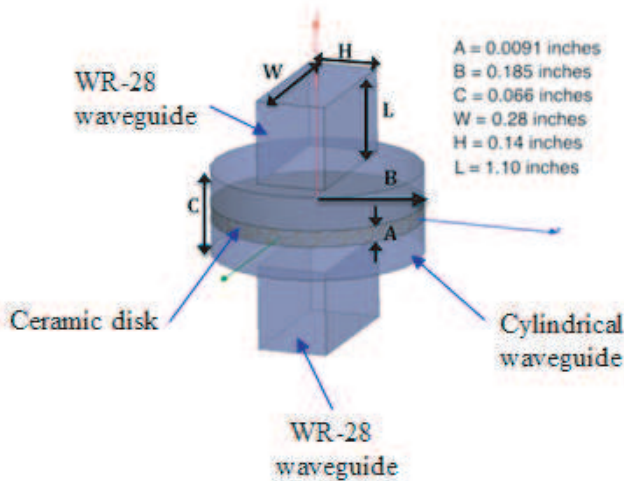


**Figure 1.** Schematic diagram of the pillbox window. Cylindrical waveguide is located between two symmetrically shaped WR-28 waveguide. Ceramic disk inside the cylindrical waveguide is shown.

study of the pillbox window and helix-TWT circuit was performed to determine the load and source impedances, respectively. The pillbox window and the helix-TWT circuit were modeled to operate across the frequency range of 30 to 34 GHz for radar applications. The pillbox window consists of an aluminum nitride ceramic disk placed at the center of the cylindrical waveguide that transitions to a rectangular waveguide of standard WR-28 dimensions at both ends. A ceramic disk with a dielectric constant of 8.4 was chosen due to its low loss tangent properties and ease of manufacturing. The height of the WR-28 rectangular waveguide and the gradual cylindrical waveguide transition were optimized to provide efficient coupling of the  $TE_{10}$  rectangular mode to the linearly polarized  $TE_{11}$  circular mode. Figure 1 shows the pillbox window that serves as the load impedance. The helix-TWT includes a cylindrical vacuum tube, a tungsten helix coil, and three beryllium oxide support rods that are placed around the helix coil with each rod oriented  $120^\circ$  apart. To ensure a strong contact between the support rods and helix coil, a thin boundary condition of gold material was placed between the flat portion of the rod and the helix coil. The helix-TWT was modeled using the single-turn approach to minimize simulation time and then optimized to fifteen turns. Figure 2 shows the helical TWT structure that serves as the source impedance.

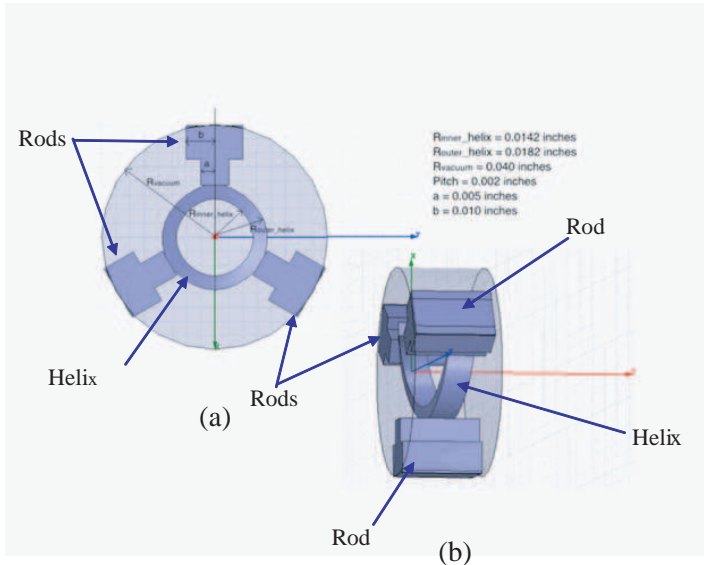


**Figure 2.** Configuration of Helix-TWT circuit showing one turn of helix coil with three supporting rods, (a) cross sectional view, (b) side view.

### 2.1. Analytic Approach

The analytical theory of transmission lines, analogous to the theory for a multi-section transformer, was used in the design. First, a transmission line was considered to be composed of several sections having differential lengths for which the impedance change by differential amounts from section to section. Then a tapered transmission line was used to match a line with normalized impedance unity to the pillbox coupler with normalized load impedance,  $Z_L$ , of 311 ohms and the helix-TWT with normalized source impedance,  $Z_0$ , of 208 ohms. The taper line has normalized impedance,  $Z$ , which is a function to the distance  $z$  along the taper. The following equations demonstrate the analytic approach for solving the Klopfenstein taper design problem [1, 2].

#### 2.1.1. Theory of Small Reflection

For a transmission line shown in Figure 3, the reflection coefficient of a gradual impedance tapered line can be determined using the theory of small reflection and is expressed as [1]

$$\Gamma(\theta) = \frac{1}{2} \int_{z=0}^L e^{-2j\beta z} \frac{d}{dz} \ln \left( \frac{Z}{Z_0} \right) dz \tag{1}$$

where  $Z_0$  represents the reference impedance at the input end of the taper upon which the reflection coefficient is defined,  $z$  is the position along the taper,  $L$  is the taper length,  $\beta$  is the propagation constant,  $\theta$  is the phase response from position 0 to  $z$ , and  $\theta = \int_0^z 2\beta dz'$ . This

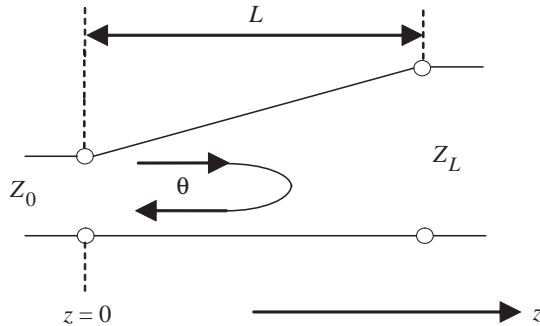


**Figure 3.** Schematic of impedance transformation between transmission line of length  $L$ .

implies that if the impedance value at each point along the tapered line is known, the reflection coefficient can be determined based on (1).

2.1.2. The Klopfenstein Taper

We first observe the Klopfenstein impedance taper for TEM structures to be optimum in the sense that the reflection coefficient is minimized over the passband [1]. With pre-designated minimum reflection coefficient in the passband  $\Gamma_m$ , taper length  $L$ , input impedance  $Z_0$ , and load impedance  $Z_L$ , the logarithm of the characteristic impedance variation for the Klopfenstein taper is given by

$$\ln Z(z) = \frac{1}{2} \ln Z_0 Z_L + \Gamma_m A^2 \phi \left( \frac{2z}{L} - 1, A \right), \quad \text{for } 0 \leq z \leq L \quad (2)$$

where

$$A = \cosh^{-1} \left( \frac{\Gamma_0}{\Gamma_m} \right) \quad (3)$$

$$\Gamma_0 = \frac{1}{2} \ln \left( \frac{Z_L}{Z_0} \right) \quad (4)$$

$$\Gamma_m = \frac{\Gamma_0}{\cosh A} \quad (5)$$

and the function  $\phi(z, A)$  is defined as

$$\phi(z, A) = -\phi(-z, A) = \int_0^z \frac{I_1 \left( A\sqrt{1-y^2} \right)}{A\sqrt{1-y^2}} dy, \quad \text{for } |z| < 1 \quad (6)$$

where  $I_1$  is the modified Bessel function which has the following special values

$$\phi(0, A) = 0 \quad (7)$$

$$\phi(z, 0) = \frac{z}{2} \quad (8)$$

$$\phi(1, A) = \frac{\cosh A - 1}{A^2} \quad (9)$$

The reflection coefficient is given by

$$\Gamma(\theta) = \Gamma_0 e^{-j\beta L} \frac{\cos \sqrt{(\beta L)^2 - A^2}}{\cosh A} \quad \text{for } \beta L > A \quad (10)$$

and

$$\Gamma(\theta) = \Gamma_0 e^{-j\beta L} \frac{\cos \sqrt{A^2 - (\beta L)^2}}{\cosh A} \quad \text{for } \beta L < A \quad (11)$$

where  $\theta$  is the electrical length.

The reflection coefficient at zero frequency is given by

$$\Gamma_0 = \frac{Z_L - Z_0}{Z_L + Z_0} \cong \frac{1}{2} \ln \left( \frac{Z_L}{Z_0} \right) \quad (12)$$

The maximum ripple in the passband is governed by  $\Gamma_m$  defined by (5).

Observation of the Klopfenstein taper design reveals a lower-end cutoff frequency at the passband, while no upper-end cutoff frequency exists as defined in the relationship of  $\beta L > A$ . The cutoff frequency decreases when either the taper length increases (may not be desired for microwave circuit design) or the value of the factor  $A$  decreases. As described in (3) and (4), the larger the ratio of impedance transformation  $Z_L/Z_0$  and the smaller the minimum reflection coefficient,  $\Gamma_m$ , the higher the cutoff frequency,  $f_c$ , with increasing  $A$ . Generally, these factors act counter conducive of each other, so one factor may have to compromise in order to achieve the other for certain desired performance.

## 2.2. Design Methodology — Optimal Taper for Non-TEM Waveguide Structures

Although the Klopfenstein taper was proposed with intended applications for TEM structures, where the propagation constant  $\beta$  is non-dispersive and the characteristic impedance is well defined, modifications needed to be made in order to make use of the concept of Klopfenstein taper for non-TEM structures. Given the physical dimensions of the input and output ports, along with the specified bandwidth and return loss parameters, the shape of the taper can be realized. Using the relationship described in (1) makes it possible to find the input reflection coefficient of the gradual impedance taper for a non-TEM line as follows

$$\Gamma_{in}(f) = \frac{1}{2} \int_0^{\theta_t} e^{-j\theta} \frac{d}{d\theta} \ln \left( \frac{Z(\theta)}{Z_0} \right) d\theta \quad (13)$$

where

$$\theta(f, z) = \int_0^z 2\beta(f, z') dz' \quad (14)$$

is the phase response to a point  $z$  along the taper and the total phase delay as  $\theta_t = \theta(f, L)$ . The function  $Z(\theta)$  is the modified characteristic impedance variation along the non-TEM taper, and is an implicit

function of  $z$ . In order to maintain an input reflection coefficient  $\Gamma < \Gamma_m$  over the desired bandwidth, it has been shown [1, 2] that  $Z(\theta)$  can be calculated as follows

$$\ln\left(\frac{Z(\theta)}{Z_0}\right) = \frac{1}{2} \ln\left(\frac{Z_L}{Z_0}\right) + \Gamma_m A^2 \phi\left(\frac{2\theta}{\theta_t} - 1, A\right) \quad (15)$$

where the passband is defined as  $\theta_t > 2A$ . Given that for a non-TEM structure, the propagation constant,  $\beta$ , becomes dispersive and the phase response,  $\theta$ , is no longer a linear function of  $\beta$  and  $z$  we can assume that  $\beta$  is a monotonically increasing function of frequency and make the lowest operating frequency defined by

$$\theta_t(f_c) = 2A \quad (16)$$

which is an implicit relationship between the taper length,  $L$ , the lower cutoff frequency,  $f_c$ , and the maximum reflection coefficient,  $\Gamma_m$ .

The main difficulties in applying the above results are the frequency dependence of the wave impedance and propagation constant, coupled with the difficulty in translating the impedance as a function of  $\theta$  into a function of  $z$  and subsequently in determining the physical parameters required to design the Klopfenstein taper. Moreover, the frequency dependence of the wave impedance and propagation constant means that the result in (15) would require a different physical taper at each frequency. However, since the dominant mode along the rectangular waveguide is found to be TE in nature, the relationship between the wave impedance and propagation constant can be evaluated as

$$Z = \frac{\omega\mu}{\beta} \quad (17)$$

then (15) can be rewritten in terms of  $\beta$

$$\beta(f, z) = \sqrt{\beta_L \beta_0} \exp\left[-\Gamma_m A^2 \phi\left(\frac{2\theta(f, z)}{\theta_t} - 1, A\right)\right] \quad (18)$$

where  $\beta$ ,  $\beta_L$  and  $\beta_0$  correspond to  $Z$ ,  $Z_L$  and  $Z_0$ , respectively using (16). To compute the required propagation constant as a function of the position along the taper  $\beta(z)$ , the taper structure is divided into  $N$  sections of length  $\Delta z = L/N$ , and  $\theta$  can be approximated as

$$\theta(z_i) = \sum_{k=0}^{i-1} 2\beta(z_k) \Delta z = \theta(z_{i-1}) \Delta z \quad (19)$$

where  $N$  must be large enough to ensure good approximation.

In the design process, the characteristic impedance at each end of the taper line was first determined by taking the previous design

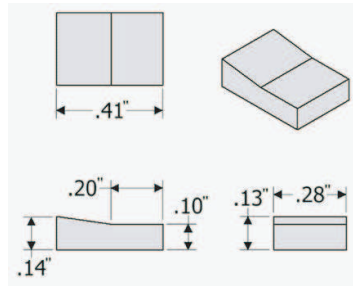


**Figure 4.** Schematic diagram of the Klopfenstein tapered transformer showing the inner dimensions.

for the pillbox window and helical structure, and recalculating the dimensions for Ka-band operation. Then, with an initial guess of  $\theta_t$  and  $\theta(Z_0) = 0$ ,  $\beta(Z_0)$  can be calculated from (18) and  $\theta(Z_1)$  can be determined from (19). By repeating the same process, all the values of  $\theta(Z_i)$  and  $\beta(Z_i)$  with  $i = 1$  to  $N$  can be computed. The iterative process continues until the solution set of  $\beta$  converges and the shape of the optimal taper is determined. Typically, a different physical taper is required for each different frequency due to the frequency dependence of the propagation constant, making it exhaustive to implement. Therefore, the center frequency at the band of interest was chosen as the operating frequency for the tapered design.

In the proposed Klopfenstein transformer, the impedance curve was segmented into 21 sections, which were then placed in transmission line rendering 21 line widths. The 21 sections were employed since these provided good convergences in the solution set of  $\beta$ . These line widths were then placed at equal intervals to the end of the pillbox WR-28 rectangular waveguide creating a piecewise metal taper. There is not a length requirement associated with this taper design, as any physical length to wavelength relationship is not relevant. Therefore, the shortest possible length was chosen that fits manufacturing guidelines. The discontinuities of the segmented sections are handled by smoothing the rigid edges to create a continuous taper and help further mitigate reflections seen by the boundary. The inner dimensions and configurations of the Klopfenstein taper design is shown in Figure 4.

### 2.3. Simulation

The proposed Klopfenstein transformer with the pillbox window and helix-TWT was simulated in order to obtain accurate prediction of

*S*-parameters. A 3-D finite element analysis tool Ansoft HFSS (High Frequency Structure Simulator) [3] was used for in frequency range of 30 to 34 GHz. The Klopfenstein transformer was located between the helix-TWT structure and pillbox window. The final configuration was optimized for minimum reflections and loss. A complete schematic of the simulated configuration is shown in Figure 5. The results from the simulation show that  $S_{11}$  is below  $-25$  dB, and  $S_{21}$  is better than  $-0.08$  dB from 30 to 34 GHz. The lowest reflection for  $S_{11}$  was  $-54$  dB at 34 GHz, and the best transmission for  $S_{21}$  was  $-0.033$  dB at 30.5 GHz. Simulation of pillbox window and Klopfenstein

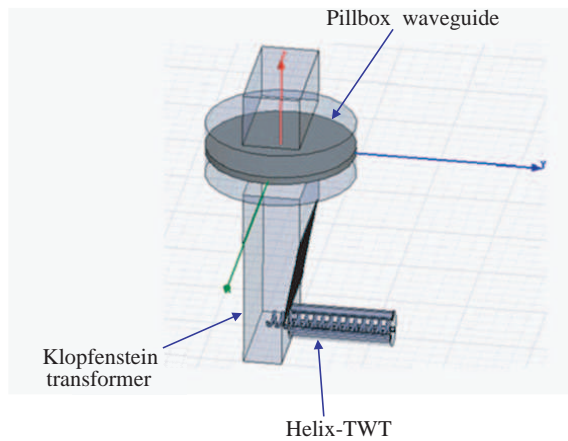


**Figure 5.** Schematic of the pillbox window, Klopfenstein transformer, and helical TWT design used in simulation.

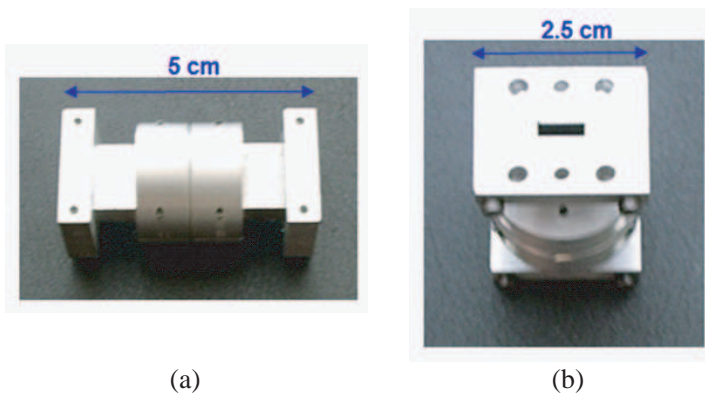


**Figure 6.** Fabricated Klopfenstein transformer with pillbox coupler, (a) side view, (b) top view.

transformer excluding the helix-TWT circuit was also performed. The simulation results showed same results as when the helix-TWT circuit was included.

### 3. MEASURED RESULTS AND DISCUSSION

The proposed Klopfenstein transformer and pillbox window assembly were fabricated, and the measurements were performed by connecting

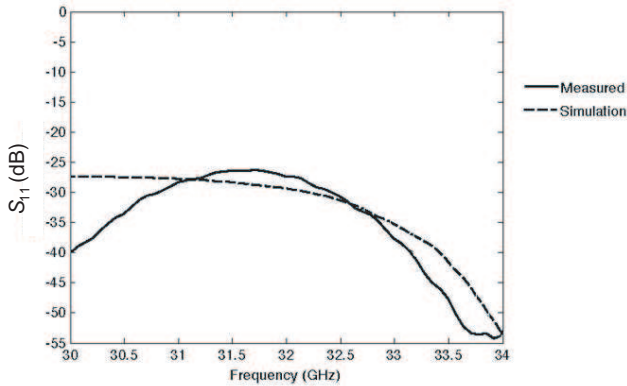


**Figure 7.** Simulated and measured  $S_{11}$  of the Klopfenstein transformer with pillbox window.

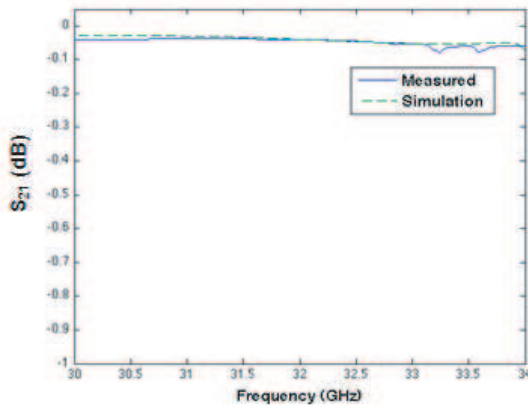


**Figure 8.** Simulated and measured  $S_{21}$  of the Klopfenstein transformer with pillbox window.

two identical structures in back-to-back configuration. To simplify fabrication process, helix-TWT was not included in fabricated transformer assembly. The fabricated transformer is shown in Figure 6. Measurements were performed using the two-port Agilent E8364A vector network analyzer. Comparisons of the measured and simulated results are shown in Figures 7 and 8. The measured results are in good agreement with the simulated ones.

#### 4. SUMMARY AND CONCLUSION

In this paper, the  $S$ -parameters  $S_{11}$  and  $S_{21}$  of a Klopfenstein transformer waveguide for matching the impedances of a Ka-band pillbox window and helix-TWT were investigated, and the results have been presented. The tapered waveguide was designed and optimized using 21 piecewise sections to create the tapered line. Simulation results showed  $S_{11}$  to be less than  $-25$  dB and  $S_{21}$  better than  $-0.08$  dB across 30 to 34 GHz. The measured results agreed closely with simulation. The Klopfenstein transformer developed in this work can be used for helix-TWT amplifiers for high power radar applications.

#### ACKNOWLEDGMENT

The authors would like to thank Tom Mulcahy for his help on the  $S$ -parameters measurements and Calvin Roberts for manufacturing the prototype.

#### REFERENCES

1. Pozar, D. M., *Microwave Engineering*, John Wiley & Sons, 2005.
2. Klopfenstein, R. W., "A transmission line taper of improved design," *Proc. IRE*, Vol. 44, 31–35, 1956.
3. <http://www.ansoft.com/products/hf/hfss/>.